Grasp Quality Evaluation and Planning for Objects with Negative Curvature

Shuo Liu Zhe Hu Hao Zhang Mingu Kwon Zhikang Wang Yi Xu Stefano Carpin

***Abstract*— We consider the problem of grasping concave objects, i.e., objects whose surface includes regions with negative curvature. When a multifingered hand is used to restrain these objects, these areas can be advantageously used to determine grasps capable of more robustly resisting to external disturbance wrenches. We propose a new grasp quality metric specifically suited for this case, and we use it to inform a grasp planner searching the space of possible grasps. Our findings are validated both in simulation and on a real robot system executing a bin picking task. Experimental validation shows that our method is more effective than those not explicitly considering negative curvature.**

I. INTRODUCTION

The problems of grasp quality evaluation and grasp planning are inherently intertwined. Grasp planning is often performed as an informed search process in the space of possible grasps, and grasp quality is used as the metric to inform the search. The ability to restrain an object despite external disturbance wrenches is greatly desirable in numerous applications, and this led to the concept of *force closure* grasp, i.e., a grasp capable of resisting an arbitrary external disturbance wrench. Consequently, numerous grasp quality metrics have been proposed in literature to evaluate this ability (see Section II for references.) Most grasp quality metrics, however, just consider the normal component of the force exerted at a contact point and do not take into account the surface local to the point where the force is applied. Figure 1 illustrates this situation in the simpler case of planar objects. The leftmost figure shows a concave object and the blue dots indicate two contact points for a possible grasp. Similarly, the rightmost figure illustrates a convex object and the blue dots also indicate two contact points for a grasp. Most grasp quality metrics would rank these two grasps as equivalent because, as shown in the middle figure, locally the two surfaces coincide and therefore the same grasp wrench space is generated. Real world experience and common sense however indicate that the one on the left is more stable, i.e., it will be capable of resisting disturbance wrenches of higher magnitude (think for example to a disturbance force acting vertically on the middle of the lower edge of both objects.) This effect is magnified if we also consider that in practice contacts hardly occur at just one point.

Shuo Liu and Stefano Carpin are with the University of California, Merced, USA. Zhe Hu, Hao Zhang, Mingu Kwon, Zhikang Wang and Yi Xu are with Dorabot Inc., Shenzhen, China.

S. Liu and S. Carpin are partially supported by NIST under cooperative agreement 70NANB12H143. Any opinions, findings, and conclusions or recommendations expressed in these materials are those of the authors and should not be interpreted as representing the official policies, either expressly or implied, of the funding agencies of the U.S. Government.

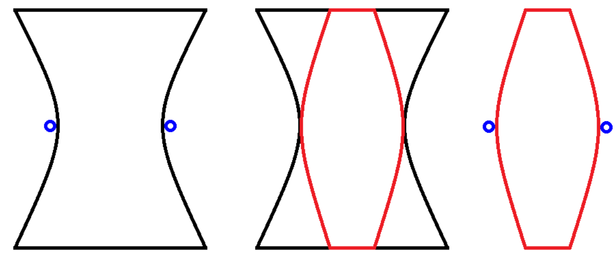

Fig. 1. Subfigure (a) shows two grasping points on the surface of a concave planar object, whereas subfigure (c) considers a convex planar object. Subfigure (b) in the middle show that the normals at the grasping points are identical.

The simple example we just illustrated motivates the contribution presented in this paper, i.e., the idea of integrating the surface geometry into the grasp quality metric through the friction cone. More precisely, we start with the development of a grasp quality metric specifically conceived for objects featuring negative curvature boundaries, i.e., concave objects. This metric overcomes classical approaches exclusively considering normals at the contact point but ignoring the curvature of the local neighborhood to the contact point. This idea builds upon the known concept of second order force and form closure considered in literature. Then, we use this new metric to inform a grasp planner that actively seeks to exploit negative curvature regions when considering concave objects to grasp.

The rest of the paper is structured as follows. Related work is presented in Section II, while in Section III we introduce relevant mathematical background. In Section IV we formalize the concept of curvature dependent grasp quality metric, and we sketch how this can be used for grasp planning. The approach is demonstrated in simulation and on a real robotic arm with a multifingered robotic hand in Section V. Finally, we draw conclusions and outline future work in Section VI.

II. RELATED WORK

Due to their practical importance to implement efficient grasp planners, grasp quality metrics have been extensively studied in the past. A recent survey by Roa and Suárez [16] offers a comprehensive summary of twenty-four metrics proposed through the years, and reveals that negative curvature is normally not considered. Despite the fact that many different metrics have been proposed in literature, very few are considered in practice. The metric perhaps most used in practice was proposed by Ferrari and Canny more than twenty years ago [4] and evaluates a grasp based on its ability to resist an arbitrary external disturbance wrench. To this end, it exclusively considers the normal component of the force at the contact point. This metric became popular because it is intuitive and relatively simple to determine, since it boils down to the computation of a six dimensional convex hull. However, it is not immune from drawbacks. For example, it is not scale invariant, and its numeric value depends on an arbitrarily chosen origin point to compute torques. Perhaps most importantly from a practical standpoint, the metric considers the ability to resist arbitrary external wrenches, while in reality disturbance wrenches are almost invariably due to disturbance forces. In an effort to overcome the limitations of this approach, methods considering only disturbances occurring in practice were proposed [1], [18]. The metrics, however, still do not consider the local curvature of the object being grasped, and did not become very popular because of their computational burden. Recently, we proposed two algorithms to significantly expedite the computation of these metrics [7], [8], but these contributions do not alter their definition and therefore do not consider the local curvature of the object at the grasping point.

The idea of explicitly considering negative curvature in grasp quality evaluation is related to second order force and form closure, a concept well known in literature [14], [15]. However, grasp metrics directly related to this concept are not popular. The idea of exploiting concavities to better restrain an object has also been considered already, especially for form closure grasps [5]. One of the few contributions that explored the area of grasping on curved parts but did not take advantage of negative curvature was proposed in [3]. Concavities on the object surface are often considered in caging, and caging grasps where the emphasis is more on form closure and on the ability to retain an object in a certain area or configuration without necessarily immobilizing it. Various studies linking caging to grasping have been proposed [17], [19], [20]. These methods, however introduce further assumptions and constraints for the shape of the object or the structure of the robotic hand, whereas we aim to develop a broadly applicable method.

III. Background

We shortly introduce some concepts related to force closure grasps. The reader is referred to [2], [12], or [14] for a comprehensive introduction to the topic. Let $\mathcal{B}$ be a rigid body to grasp using a multifingered robotic hand. We assume the commonly used point contact finger model, i.e., each finger establishes contact with $\mathcal{B}$ at a single point $\mathbf{p}$ and exerts a force $\mathbf{f}$ towards the object. We assume that the surface of $\mathcal{B}$ is differentiable in $\mathbf{p}$ and let $\mathcal{T}_\mathbf{p}$ be the tangent plane in $\mathbf{p}$. A local, right-handed orthonormal reference frame is established at the contact point $\mathbf{p}$, with two axis $\mathbf{u}$ and $\mathbf{w}$ lying on $\mathcal{T}_\mathrm{b}$ and the third axis $\mathbf{t}$ orthogonal to $\mathcal{T}_\mathbf{p}$ and pointing inwards. Let $[f_1\ f_2\ f_3]$ be the three components of $\mathbf{f}$ along $\mathbf{t}$, $\mathbf{u}$ and $\mathbf{w}$, respectively. According to the Coulomb friction model, let μ be the friction coefficient between $\mathcal{B}$ and the finger at $\mathbf{p}$. Slippage between the finger and the object does not occur as long as the force $\mathbf{f}$ belongs to the following set:

$$F(\mathbf{p}) = \left\{ \mathbf{f} \in \mathbb{R}^3 \mid f_1 \geq 0 \land \sqrt{f_2^2 + f_3^2} \leq \mu f_1 \right\}.$$

Mathematically, $F(\mathbf{p})$ describes a cone and it is therefore called *friction cone* at point $\mathbf{p}$. The first condition implies that the force $\mathbf{f}$ is directed inside the object, while the second condition relates the intensities of the tangential and orthogonal components. From a practical perspective $F(\mathbf{p})$ is often approximated with a regular pyramid (see Figure 2) and the force $\mathbf{f}$ is expressed as a positive combination of the components along the edges of the pyramid, i.e., $\mathbf{f} = \sum_{j=1}^{k} \alpha_j \mathbf{f}_j$, with $\alpha_j \geq 0$.

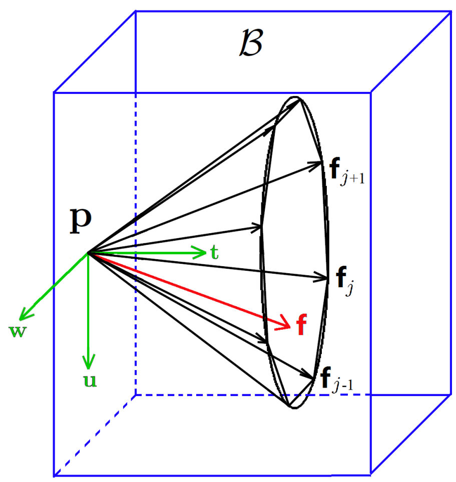

Fig. 2. Friction cone and its approximation

The grasping metrics proposed by Ferrari and Canny consider the elementary wrenches induced by force $\mathbf{f}$. The jth elementary wrench is $\mathbf{w}_j = [\mathbf{f}_j \quad \mathbf{p} \times \mathbf{f}_j]$, where the coordinates of $\mathbf{p}$ are expressed in an arbitrary reference system. The center of mass of $\mathcal{B}$ is usually chosen as origin for the reference system, but any other point is equally valid. The metrics consider the convex hull of either the union of the elementary wrenches generated by all contact points, or the convex hull of their Minkovsky sum. While the reader is referred to [4] for the precise details and definition, the intuition is that as the opening of the cone increases, the score of the grasp improves because it is capable of resisting more disturbance wrenches.

IV. Grasp Quality Metrics with Negative Curvature

In this section we develop the mathematical foundations for the grasp quality metric we propose. To explain the concepts, we use pictures displaying planar objects, but the method we develop aims at the three dimensional scenario. From an analytic perspective, differential geometry offers the pertinent tools and concepts [6], although, as we will outline in the next section, from a practical standpoint objects are most often represented using triangular meshes and therefore feature many local non-differential patches. Moreover, as we explained in the previous section, in practical scenarios most representations rely on discrete models (e.g., discretized friction cones). Therefore it will be necessary to eventually reconcile the continuous models and representations with their discrete counterparts. For the time being we assume that the boundary of the object being grasped can be decomposed as a finite collection of surfaces and that the grasping points are placed at differentiable points. That is to say that if $\mathbf{p} \in \mathbb{R}^3$ is a contact point on the surface of the object, then there exists a neighborhood of $\mathbf{p}$ such that the points $\mathbf{x}$ on the surface satisfy the equation $g(\mathbf{x}) = 0$ where $g : \mathbb{R}^3 \to \mathbb{R}$ is a suitable function twice differentiable in $\mathbf{p}$. Moreover, points inside the object are such that $g(\mathbf{x}) < 0$. To begin with, consider Figure 3. The three blue dots display three possible contact points on the surface of an object. According to our previous considerations, point number 1 and number 3 lie in a locally convex and concave patches of the surface. Therefore point number 3 is more valuable than point number 1 in terms of its ability to resist an external wrench, e.g., a wrench due to an external lateral force. Point number 2 represents an intermediate situation, whereby an orthogonal force applied there would help resist forces pushing the object up, but not down.

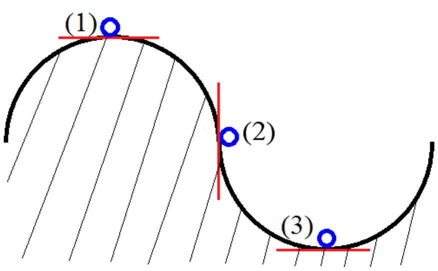

Fig. 3. Three different conditions for contact points on a curved surface bounding the object from above.

Next, consider Figure 4. All cases depict contact points in locally convex patches of the surface. However, from left to right, the local curvature increases, and then intuitively one would prefer the rightmost contact point for its ability to restrain a disturbance wrench.

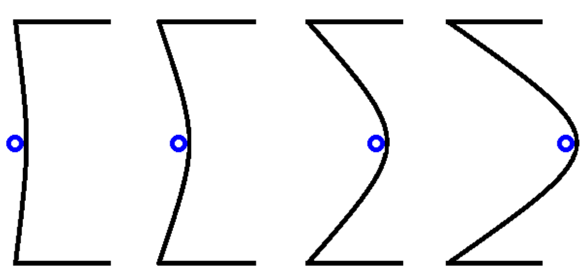

Fig. 4. Grasping points in blue on the black surface with different ratio of curvature.

Starting from the above observations, we then aim at the analytic definition of a quality metric incorporating them. The idea is to *dilate* the friction cone $F(\mathbf{p})$ at the contact point considering the local curvature of the surface at the contact point. According to our assumptions, the Hessian matrix of the function g at $\mathbf{p}$ exists. Let $\mathbf{H}(\mathbf{p})$ be such matrix. The local concavity or convexity of g in $\mathbf{p}$ can be determined from the properties of $\mathbf{H}(\mathbf{p})$. If g is locally convex, then the friction cone remains unchanged, as suggested by the first contact point in Figure 3. If g is instead locally concave, then the friction cone should be expanded, as for the third contact point in Figure 3. Such expansion should not be isotropic (i.e., uniform), but rather dependent on the local curvature. That is to say that the friction cone should be expanded more towards the directions in which g grows more, and viceversa. Different surface curvature measures have been proposed in differential geometry. However, aiming at a definition that can be turned into an easy to compute method, we instead estimate the curvature, and then the expansion of the friction code, considering *directional slices* of the function g. Let $\mathbf{v}$ be a unit length vector on the tangent plane $\mathcal{T}_\mathbf{p}$, and let $g_\mathbf{v}$ be the unidimensional function obtained evaluating g along the direction identified by $\mathbf{v}$. For a given small constant h, we therefore define

$$\nabla g'_\mathbf{v} = \frac{g'(\mathbf{x} + h\mathbf{v}) - g'(\mathbf{x})}{h}$$

where g' is a well defined derivative of the single variable function g evaluated along $\mathbf{v}$. Note that h is a constant for a given hand, but will in general vary for different hands, i.e., be a function of the finger size. From an algorithmic standpoint this can be achieved considering a few directions on the plane tangent to g in $\mathbf{p}$ and then computing the $\nabla g'_\mathbf{v}$ along these directions. Directions can be uniformly spaced or randomly selected. The same idea can be applied when g is locally concave, convex, or neither convex nor concave (e.g., a saddle point). In each case the friction cone $F(\mathbf{p})$ is expanded exclusively in the directions along which $\nabla g'_\mathbf{v}$ is positive. This idea can be formalized as follows. For a given force $\mathbf{f}$, let $\mathbf{v_f}$ be the unit length vector lying in $\mathcal{T}_\mathbf{p}$ and having the same direction defined by f_2 and f_3. In the frame $\mathbf{t}, \mathbf{u}, \mathbf{w}$, $\mathbf{v_f}$ is then[1]

$$\mathbf{v_f} = \begin{bmatrix} 0 & \frac{f_2}{\sqrt{f_2^2 + f_3^2}} & \frac{f_3}{\sqrt{f_2^2 + f_3^2}} \end{bmatrix}.$$

We then define the expanded friction cone $F^E(\mathbf{p})$ as

$$F^E(\mathbf{p}) = \begin{cases} \mathbf{f} \mid \sqrt{f_2^2 + f_3^2} \leq \mu f_1 & \text{if } \nabla g'_\mathbf{v_f}(\mathbf{p}) \leq 0 \\ \mathbf{f} \mid \sqrt{f_2^2 + f_3^2} \leq (\mu + \zeta) f_1 & \text{if } \nabla g'_\mathbf{v_f}(\mathbf{p}) > 0 \end{cases}$$

Where $\zeta = k \nabla g'_\mathbf{v_f}(\mathbf{p})$ and k is a fixed parameter $k > 0$. In particular, since the same k is used to perform alternative grasps for the same object, the relative score is rather insensitive to k as long as it is positive. Note that in this definition we did not write the condition $f_1 \geq 0$ in the interest of space, but this should be nevertheless assumed.

[1]Recall that the first component is along the orthogonal axis $\mathbf{t}$.

The newly defined $F^E(\mathbf{p})$ formally captures the cases intuitively discussed in Figure 3 and 4, i.e., it expands $F(\mathbf{p})$ only along directions of negative curvature, and it moreover performs an anisotropic expansion, i.e., the cone is grown more in the directions of larger negative curvature. Note that from a geometric standpoint, $F^E(\mathbf{p})$ is still a cone albeit its base is no longer circular.

From a practical perspective, as we mentioned in the previous section, the friction cone $F(\mathbf{p})$ is most often represented by a regular pyramid. Moreover, as explained in the next section, the directional derivative is evaluated only along a finite number of directions. A convenient approach is to evaluate directional derivatives only along directions orthogonal to the pyramid edges and to then expand only the edges associated with directions revealing negative curvatures.

A. *Grasp Planner using Negative Curvature*

In this subsection we describe a grasp planner using the grasp quality metric we just presented to inform its search through the space of possible grasps. While the underlying principles are general, aiming at the validation of the robot on our existing robotic hardware, some implementation choices are made considering the hardware we will use. In particular we focus on the multifingered Dora Hand produced by Dorabot, Inc., whose CAD rendering is shown in figure 5. Note that while the fingers can be closed, they cannot be moved around the palm of the hand, and therefore the relative position of their first joint remains constant. The finger on the left of the figure is indicated as *finger 1* in the following.

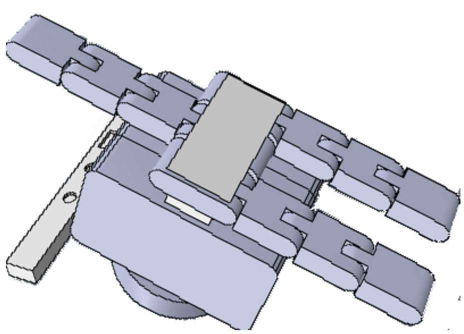

Fig. 5. Dora Hand model.

As formerly stated, in most scenarios objects are represented using triangular meshes. This is very often true also when considering objects with curved surfaces, since they can be modeled as a large collection of small size triangles. In the following, we indeed hypothesize that the objects' surface is represented by meshes of triangles, and it is therefore necessary to appropriately adapt the general concepts we developed assuming differential surfaces.

The planner starts locating all edges whose adjacent faces form a concave region. Figure 6 shows some examples, with such edges shown in red, while the normals of the two adjacent faces are shown in green and blue.

The planner we developed is inspired by the approach presented in GraspIt! [11], i.e., it randomly generates hand positions around the object to be grasped and then determines the contact points by simulating finger closing. Eventually, the grasp with the highest value for the grasping metric is returned. This general idea is adapted for the hand we consider as follows. First, a point of negative curvature is determined on the triangular mesh and a hand configuration is generated so that the finger 1 makes contact with such point. Once the contact point of the first finger is determined, the joint space of the finger is sampled to determine a set of end-effector poses, and from those poses we determine the contact points for the other two fingers by projecting how they would close. This is very similar to what is done in GraspIt! and many other planners. End-effector configurations that do not yield three contact points are discarded. At this point the quality of the remaining grasp configurations is determined. The process is then repeated multiple times, and at each iteration a new point with negative curvature is randomly chosen.

Figure 7 shows some example grasps computed by the planner we just described. Note that the finger 1 always makes contact on the surface with negative curvature.

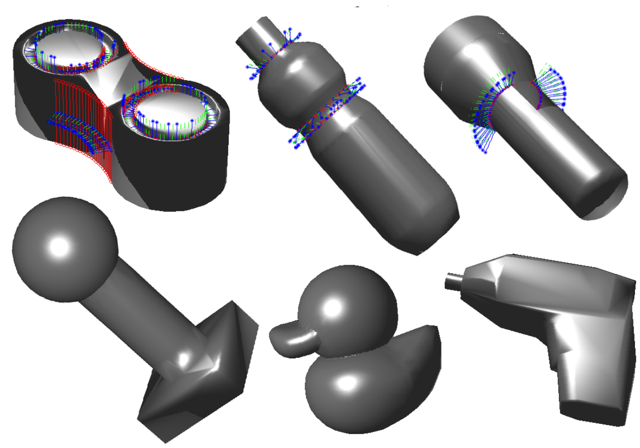

Fig. 6. Examples of the objects we used in simulation. The top row also shows the negative curvature attached to edges in red lines. Blue and green lines are the normal vector of the two adjacent faces connected by the negative curve edge.

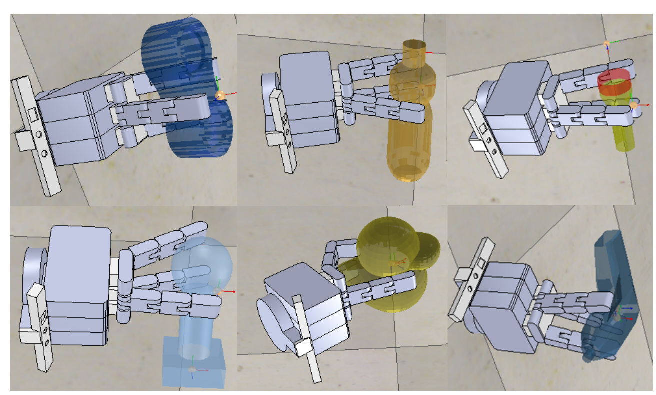

Fig. 7. Grasps determined by the grasp planner for six different objects.

V. Experiments and Results

In this section we present some results illustrating the metric we proposed in this paper and we show how it informs a planner performing a bin picking task using a commercially available robot.

A. Preliminary Results

Revisiting Figures 3 and 4, our first experiment shows the effect in grasp quality with respect to the ratio of negative curvature. In the following we consider two quality measures, namely the Ferrari-Canny metric formerly discussed, and the volume of the grasp wrench space [10]. This metric is indicated as V_{GVS}. The reason to consider also this second metric will become clear later on in this section. We consider objects similar to Figure 1(a), where the curve is generated by the function $x_-(y) = -\alpha y^2 - c$ and $x_+(y) = \alpha y^2 + c$. By varying y within $[-y_0, y_0]$, we obtain an object with the center of mass located at $(0, 0)$. We fix our grasp point $\mathbf{p_1}$ at $(-c, 0)$ and $\mathbf{p_2}$ $(c, 0)$. Therefore, we use the expanded friction cone $F^E(\mathbf{p_1})$ and $F^E(\mathbf{p_2})$ to calculate the grasp wrench space.
The top row in Figure 8 shows an example with $c = 2$, $k = 0.05$ and $\alpha = 0, 2, 4$. We approximate $\nabla g'_{\mathbf{v_f}}(\mathbf{p})$ with $h = 0.001$, so that $\nabla g'_{\mathbf{v_f}}(\mathbf{p}) = 2\alpha$. The Ferrari-Canny quality and grasp wrench space volume are indicated below each object. The examples show that in this case both metrics are increased as the curvature of the object increases and the friction cone is correspondingly expanded. Figure 9 displays the relationship between the Ferrari-Canny grasp quality and the curvature.

Next, we consider a situation similar to point (2) in Figure 3. In this case the curve is generated by function $x_-(y) = \alpha y^3 - c$ and $x_+(y) = \alpha y^3 + c$, with y within $[-y_0, y_0]$. The center of mass is still located at $(0, 0)$ and we fix our grasp points at $\mathbf{p_1}$ at $(-c, 0)$ and $\mathbf{p_2}$ $(c, 0)$. Then, we use the expanded friction cone $F^E(\mathbf{p_1})$ and $F^E(\mathbf{p_2})$ to calculate the grasp wrench space. The bottom row in Figure 8 shows some examples with with $c = 2$, $k = 33.33$ and $\alpha = 0, 2, 4$. We approximate $\nabla g'_{\mathbf{v_f}}(\mathbf{p})$ with $h = 0.001$, so that $\nabla g'_{\mathbf{v_f}}(\mathbf{p}) = 0.003\alpha$. As for the previous examples, the values for both the Ferrari-Canny and V_{GWS} metrics are shown. These last examples show why we considered V_{GWS}, too. In this case the Ferrari-Canny metric does not change because it is defined by the worst case disturbance. In this case the asymmetric expansion of the friction cone helps in resisting disturbance forces, but is neutral with respect to a disturbance torque rotating the object counterclockwise. This is consistent with the metric definition, but is indeed one of the weaknesses of this metric, i.e., it is defined by worst case scenarios that may hardly occur in practice. On the contrary, the metric considering the volume of the grasp wrench space grows, indicating that the grasp can resist a wider range of force disturbances.

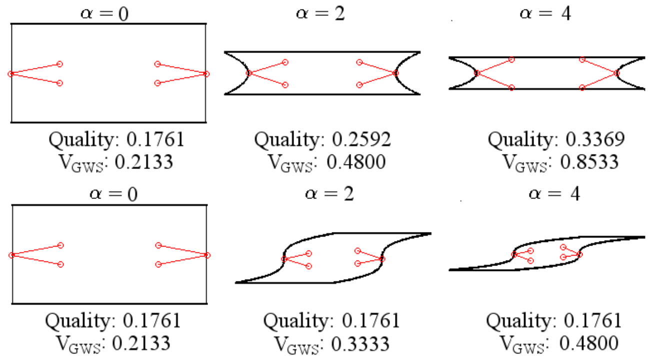

Fig. 8. 2D example on objects with different contacting curvature. Red line shows the expanded friction cone at the contact point.

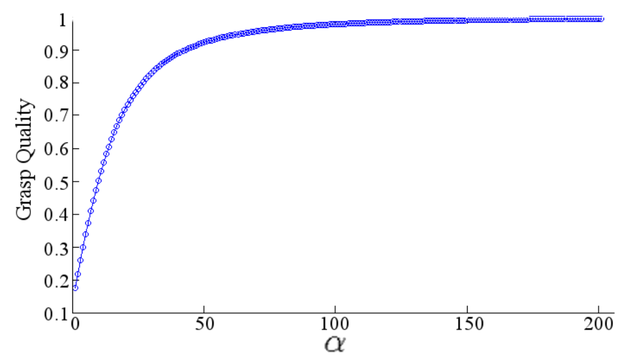

Fig. 9. The relationship between grasp quality and the curvature of the surface for setup shown in figure 8.

B. Grasp Planning Comparison

To show how the grasp planner we developed takes advantage of negative curvatures, we compare it with a baseline random grasp planner, as it is often done in literature [9], [13]. In the following, our planner is referred to as *NC* planner, where *NC* stands for negative curvature. The random grasp planner was implemented by simply giving a random pose of the object with respect to the hand, then close the hand based of its hardware structure and measure the quality of the grasp. This is basically the GraspIt! approach.
We chose the 3 objects shown in Figure 6, i.e. a duck, a bottle and an eight-shaped object representing the logo of Dorabot, Inc., (referred to as DoraLogo in the following). Figure 10 shows the comparison result between our grasp planer and the random grasp planner with both of them generating the same amount of grasps. The time spent to generate grasps using our NC grasp planner and the random planner is shown in Table I. Clearly, our NC grasp planner is more efficient in generating grasps with higher quality.

For fairness, it is also important to notice that the NC grasp planner has some limitations. First, it offers no advantages if the object to be grasped has not negative curvature areas. In addition being biased towards areas of negative curvature, if the center of mass of the object is far from these areas, the planner may produce a low quality grasp.

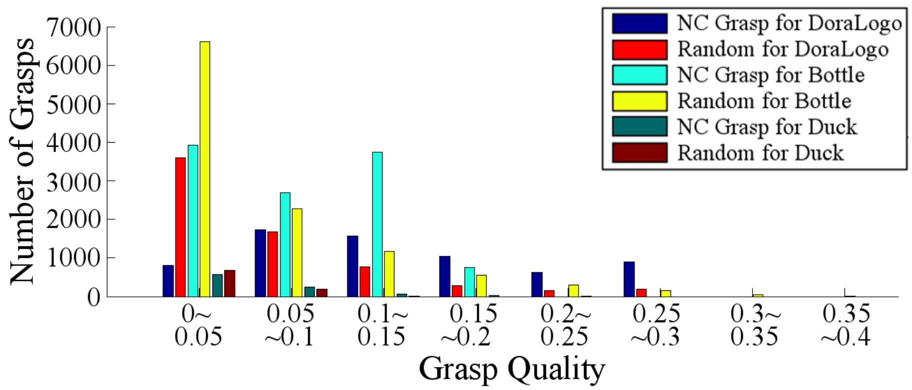

Fig. 10. Grasp quality comparison with same amount of grasps for 3 different objects.

Object	DoraLogo		Bottle		Duck	
Grasp planner	NC	Rand	NC	Rand	NC	Rand
Avg Time(s)	4.974	8.735	0.832	5.523	2.535	13.715

TABLE I
COMPARISON RESULT FOR TIME TO GENERATE GRASPS IN SIMULATION.

C. Real Robot Comparison

We conclude the validation of the method we proposed using a Dorabot mobile manipulator (see Figure 11). This robot features an omni-directional mobile base with 360 degree coverage by a lidar sensor, and it includes a lifter, a UR5 robot arm, and a reconfigurable dexterous robot hand with an eye-in-hand RGBD vision sensor. The platform can be controlled using ROS. The hand is designed in a modular fashion, and all flanges in the fingers are the same module. Each joint may be actuated or not. Each finger can have any number of flanges, and a hand can have any number of fingers. Every finger can bend in any direction, and all flanges are equipped with tactile sensors and a joint angle sensor. The hand can then function in multiple ways, from a from parallel jaw gripper to an anthropomorphic mode. The software pipeline is shown in Figure 12, and our grasp planer result intervenes in the third step—retrieving grasp from database. In this section, we show the real robot performance while grasping objsect with and without negative curvature. The objects we used to perform our test are shown in Figure 13.

We run 10 grasp test on each object with the database generated with NC grasp planner and a random grasp planner. Successful runs are determined by fully grasping the object from the bin, picking it up, and dropping the object at a predefined location, while failure is defined as not being able to complete the whole process. Failure is typically caused by the object sliding during motion or being unable to determine an appropriate grasp configuration. Figure 14 shows successful grasps for each object with our NC grasp planner whereas table II shows the overall result. The accompanying video shows the whole system in action.

The NC grasp planner clearly outperforms the grasps from the baseline random grasp planner. Since sliding may occur while the object is moved, grasping on a negative curve can better restrain the object, so we get fewer failures caused by sliding.

Fig. 11. Robot hardware

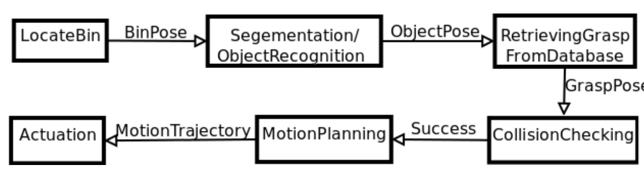

Fig. 12. Software pipeline.

Object	DoraLogo		Bottle		Duck	
Grasp planner	NC	Rand	NC	Rand	NC	Rand
Success	8	4	6	5	7	4
Success (sliding)	1	1	2	1	0	0
Fail (sliding)	1	2	0	1	3	4
Fail (motion planning)	0	3	2	3	0	2

TABLE II
COMPARISON RESULT FOR REAL ROBOT EXPERIMENT.

Fig. 13. Objects used in real robot example.

Fig. 14. Grasp example with real robot.

VI. Conclusions

In this paper we considered the problem of grasping objects with negative curvature and the related problem of evaluating grasp configurations where the fingers make contact in points of negative curvature. We proposed a modified grasp quality metric that accounts for local curvatures and shown that it overcomes many of the problems associated with commonly used metrics. The metric was then used to inform a grasp planner aiming at making contact with the object at convex areas. The method we proposed has been contrasted with a baseline planner using randomized grasps commonly used in literature and it was shown to be largely superior. Validation occurred both in simulation and on a mobile manipulator with consistent results.

References

[1] C. Borst, M. Fischer, and G. Hirzinger. Grasp planning: How to choose a suitable task wrench space. In *Proceedings of the IEEE International Conference on Robotics and Automation*, pages 319–325, 2004.

[2] S. Carpin, S. Liu, J. Falco, and K. Van Vyk. Multi-fingered robotic grasping: a primer. arXiv:1607.06620v1, 2016.

[3] B. Faverjon and J. Ponce. On computing two-finger force-closure grasps of curved 2d objects. In *Proceedings of the IEEE International Conference on Robotics and Automation*, pages 424–429, 1991.

[4] C. Ferrari and J. Canny. Planning optimal grasps. In *Proceedings of the IEEE International Conference on Robotics and Automation*, pages 2290–2295, 1992.

[5] K. G. Gopalakrishnan and K. Goldberg. Gripping parts at concave vertices. In *Proceedings of the IEEE International Conference on Robotics and Automation*, pages 1590–1596, 2002.

[6] E. Kreyszig. *Differential Geometry*. Dover, 1991.

[7] S. Liu and S. Carpin. A fast algorithm for grasp quality evaluation using the object wrench space. In *Proceedings of the IEEE International Conference on Automation Science and Engineering*, pages 558–563, 2015.

[8] S. Liu and S. Carpin. Fast grasp quality evaluation with partial convex hull computation. In *Proceedings of the IEEE International Conference on Robotics and Automation*, pages 4279–4285, 2015.

[9] S. Liu and S. Carpin. Global grasp planning using triangular meshes. In *Proceedings of the IEEE International Conference on Robotics and Automation*, pages 4904–4910, 2015.

[10] A. T. Miller and P. K. Allen. Examples of 3d grasp quality computations. In *Proceedings of the IEEE International Conference on Robotics and Automation*, pages 1240–1246, 1999.

[11] A.T. Miller and P.K. Allen. Graspit! a versatile simulator for robotic grasping. *IEEE Robotics Automation Magazine*, 11(4):110–122, 2004.

[12] R.M. Murray, Z. Li, and S.S. Sastry. *A mathematical introduction to robotic manipulation*. CRC Press, 1994.

[13] F.T. Pokorny and D. Kragic. Classical grasp quality evaluation: New theory and algorithms. In *Proceedings of the IEEE/RSJ International Conference on Intelligent Robots and Systems*, pages 3493– 3500, 2013.

[14] D. Pratticchizzo and J.C. Trinkle. Grasping. In B. Siciliano and O. Khatib, editors, *Handbook of robotics*, chapter 28, pages 671–700. Springer, 2008.

[15] E. Rimon and J. Burdick. On force and form closure for multiple finger grasps. In *Proceedings of the IEEE International Conference on Robotics and Automation*, pages 1795–1800, 1996.

[16] M. A. Roa and R. Suárez. Grasp quality measures: review and performance. *Autonomous robots*, 38(1):65–88, 2015.

[17] A. Rodriguez, M. T. Mason, and S. Ferry. From caging to grasping. *The International Journal of Robotics Research*, 31(7):886–900, 2012.

[18] M. Strandberg and B. Wahlberg. A method for grasp evaluation based on disturbance force rejection. *IEEE Transactions on Robotics*, 22(3):461–469, 2006.

[19] W. Wan, R. Fukui, M. Shimosaka, T. Sato, and Y. Kuniyoshi. Grasping by caging: A promising tool to deal with uncertainty. In *Proceedings of the IEEE International Conference on Robotics and Automation*, pages 5142–5149, 2012.

[20] W. Wan, R. Fukui, M. Shimosaka, T. Sato, and Y. Kuniyoshi. A new grasping by caging solution by using eigen-shapes and space mapping. In *Proceedings of the IEEE International Conference on Robotics and Automation*, pages 1566–1573, 2013.